



Supported by



## Accepted Article

**Title:** Diatomite Stabilized KOH: An Efficient Heterogeneous Catalyst for Cyclopentanone Self-condensation

**Authors:** Qianqian Xu, Xueru Sheng, Haiyuan Jia, Na Li, Jian Zhang, Haiqiang Shi, Meihong Niu, and Qingwei Ping

This manuscript has been accepted after peer review and appears as an Accepted Article online prior to editing, proofing, and formal publication of the final Version of Record (VoR). This work is currently citable by using the Digital Object Identifier (DOI) given below. The VoR will be published online in Early View as soon as possible and may be different to this Accepted Article as a result of editing. Readers should obtain the VoR from the journal website shown below when it is published to ensure accuracy of information. The authors are responsible for the content of this Accepted Article.

**To be cited as:** *ChemCatChem* 10.1002/cctc.202001538

**Link to VoR:** <https://doi.org/10.1002/cctc.202001538>

# Diatomite Stabilized KOH: An Efficient Heterogeneous Catalyst for Cyclopentanone Self-condensation

Qianqian Xu<sup>1</sup>, Xueru Sheng<sup>1,\*</sup>, Haiyuan Jia<sup>2</sup>, Na Li<sup>1</sup>, Jian Zhang<sup>1</sup>, Haiqiang Shi<sup>1</sup>,  
Meihong Niu<sup>1</sup>, Qingwei Ping<sup>1,\*</sup>

<sup>1</sup>*College of Light Industry and Chemical Engineering, Dalian Polytechnic University,  
Dalian 116034, Liaoning, China*

<sup>2</sup>*Shandong Provincial Key Laboratory of Molecular Engineering, School of Chemistry  
and Pharmaceutical Engineering, Qilu University of Technology — Shandong Academy  
of Sciences, No. 3501, Daxue Road, Jinan 250353, China*

Corresponding author: Xueru Sheng, Qingwei Ping

E-mail: [shengxr@dlpu.edu.cn](mailto:shengxr@dlpu.edu.cn), Tel/Fax: +86 411 86323327-603  
[pingqw@dlpu.edu.cn](mailto:pingqw@dlpu.edu.cn), Tel/Fax: +86 411 86324620

## Abstract

Aldol condensation of cyclopentanone is an attractive reaction for bio-jet fuel production. KOH is an efficient homogeneous catalyst for aldol condensation but suffering the problem of separation. In this paper, a heterogeneous catalyst, diatomite stabilized KOH (KOH/diatomite) was prepared in a simple way (dry-mixed impregnation process), and exhibited good activity (overall yield: 85.0%) and reusability. To clarify the support effect of diatomite, KOH/SiO<sub>2</sub> catalyst was also prepared. According to characterizations of these two catalysts, we suggest that the

excellent catalytic activity of KOH/diatomite can be attributed to the formation of K-O-Si bond. In addition, the impurity elements existed in diatomite (e.g. CaO, Na<sub>2</sub>O, Al<sub>2</sub>O<sub>3</sub>) and higher BET surface areas may also benefit to this reaction. This study provides a new possibility for converting homogeneous catalyst (KOH) to heterogeneous catalyst (KOH/diatomite). In this way, KOH/diatomite performed excellent catalytic activity and exhibited stable reusability, which can avoid the problem of separation and pollution.

**Key words:**

Biomass; Diatomite; Heterogeneous catalysts; KOH; Self-condensation

**1. Introduction**

With the great concern of fossil fuel and environmental issues, renewable biomass-derived fuel components conversion has gradually become an important research topic <sup>[1]</sup>. Besides, the demand of high-density jet fuel is sharply increasing in aerospace aircraft <sup>[2]</sup>. Compared with other synthesis pathways, the preparation of high-density jet fuel from renewable biomass-based materials (such as lignocellulose, starch, lipid, etc.) has been a relatively promising route <sup>[3]</sup>. Furthermore, it should be pointed out that among biomass-based materials, lignocellulose can be obtained from an economical way, such as the source of agricultural waste and forest residues. In the past years, great advances have been made in this field pioneered by Dumesic <sup>[4]</sup>, Huber <sup>[5]</sup>, Corma <sup>[6]</sup> and other researchers <sup>[7]</sup>.

Cyclopentanone is one of the biomass platforms compounds towards bio-high density fuel synthesis, which can be produced by hydrolysis, dehydration and selective

hydrogenation of hemicellulose [8]. Due to its cyclic structure and C=O groups, cyclic dimer can be produced as bio-high density fuel precursor after cyclopentanone self-condensation or with furfural aldol condensation [9]. In previous work, different homogeneous or heterogeneous catalysts were explored and used for this reaction. As for homogeneous catalysts, Wang et al. reported that KOH aqueous solution exhibited well catalytic activity (83.3%) with the mixture of Raney Co. However, KOH aqueous solution suffered the problem of subsequent separation [10]. As for heterogeneous catalysts, Deng et al. found that 98.1% selectivity of product was obtained (conversion: 46.1%) over MOF-encapsulation phosphotungstic acid [11]. Meanwhile, metal oxides catalysts also have been reported. Yang et al. reported that up to 86% yield was obtained over MgAl-HT [12]. Liang et al. showed that C10 yield reached 84.6% with 88.2% cyclopentanone conversion over MgZr41 catalyst [13]. However, the preparation process of above heterogeneous catalysts is either expensive or complex. Thus, it will be attractive to design a new heterogeneous catalyst combined KOH with supporting materials, which possesses both catalytic activity and economic efficiency.

Among various catalytic materials, finding supporting materials are higher efficiency for the conversion of cyclopentanone that is an appealing objective. Meanwhile, materials are stable to disperse loading with lower cost should be considered. Diatomite, which is derived from diatoms remains, is a natural and much cheaper material. It exhibits unique microporous structure, large specific surface area, good adsorptivity, strong acid resistance and good thermal stability [14]. Due to these characteristics,

diatomite application has been described in the literature for a lot, such as composite super absorbent <sup>[14a]</sup>, filter aids <sup>[14b]</sup>, thermal insulation materials <sup>[14c]</sup> etc. On the other hand, diatomite exhibits amorphous structure and good dispersion, which has been applied as an efficient heterogeneous catalyst support to investigate in some reactions <sup>[15]</sup>. For instance, Zhang et al. investigated the Heck and Suzuki reactions could be catalyzed by diatomite-supported Pd NPs <sup>[16]</sup>. Besides, Shan et al showed biodiesel production achieved 92.4% conversion by using diatomite-supported CaO catalyst <sup>[17]</sup>. Otherwise, Rabie et al. reported diatomite@CaO/MgO catalyst for the converting of waste cooking oil <sup>[18]</sup>.

Herein, the main goal of this contribution is to synthesis and characterize a heterogeneous diatomite stabilized KOH catalyst (KOH/diatomite), which can be further applied into cyclopentanone self-condensation. Great catalytic activity was achieved compared with KOH/SiO<sub>2</sub> catalyst.

## 2. Materials and Methods

### 2.1 Materials and catalyst preparation

#### 2.1.1 Materials

Cyclopentanone, KOH were commercial available (Sinopharm Chemical Reagent Co.,Ltd). Diatomite was collected from Changbai Mountain, Jilin, China. Fumed SiO<sub>2</sub> was obtained from Aladdin Reagent Co.,Ltd.

#### 2.1.2 Catalyst synthesis

Diatomite and KOH were mixed in a round bottom flask (500ml) with a rotor (400

r/min) at 60 °C for 24 h, which mass ratios (KOH/diatomite) range from 1:6 to 1:1. In the dry-mixed impregnation process, a magnetic heating stirrer was used to heat and mix the catalyst, and round bottom flask was fitted with frosted bottle cap. After that, the sample was calcined in muffle furnace at desired temperature (range from 300 °C to 700 °C) for 4 h. For the reusability test, after 8 h cyclopentanone self-condensation reaction, catalyst was separated from the reaction mixture and washed with ethanol solution, then calcined at 500 °C for 4 h before next reaction.

## 2.2 Characterization of catalysts

### 2.2.1 Scanning Electron Microscope (SEM) and Energy Spectrum Analysis (EDS)

The surface morphology of KOH/SiO<sub>2</sub> and KOH/diatomite catalysts was observed by SEM using JSM-7800 scanning electronic microscope. Elemental mapping scan was obtained by Energy Spectrometer X-Max50.

### 2.2.2 X-ray diffraction (XRD)

Catalysts were characterized by Shimadzu X-ray diffractometer XRD-6100. Continuous scans were collected at a step rate of 5 ° min<sup>-1</sup> with a Cu target (over a 2θ range of 10°- 80°).

### 2.2.3 Thermogravimetric Analysis (TGA).

TGA was analyzed by TGA Q500 with the temperature process of 10 °C/min raised to 700 °C.

### 2.2.4 Physical adsorption

ASAP 2020 Plus was used to measure the BET surface area at 77 K by nitrogen

physisorption. Before test, the catalysts were evacuated at 393 K for 4 h.

### 2.2.5 FT-IR spectra

The FT-IR spectra of catalysts were performed for the range from 4000  $\text{cm}^{-1}$  to 400  $\text{cm}^{-1}$  using PerkinElmer Frontier Spectrometer.

### 2.3 Activity test/ Methods

The cyclopentanone, catalysts were mixed at a mass of 4 g and 1 g respectively in a 20 mL Teflon-lined batch reactor. Before test,  $\text{N}_2$  was passed through the reactor for 30 s. Then the reactor was sealed, followed by stirring at 180  $^\circ\text{C}$  for 2 h. After that, the product was analyzed by Varian 450-GC gas chromatography.

## 3. Results and Discussion

### 3.1 Catalyst Characterization

As the major constituent of diatomite is bio- $\text{SiO}_2$ <sup>[19]</sup>, so it is ineluctable to compare the activity difference with commercial  $\text{SiO}_2$ . KOH/diatomite and KOH/ $\text{SiO}_2$  catalysts were prepared for this reaction. To investigate the structure-activity difference between KOH/ $\text{SiO}_2$  and KOH/diatomite, several characterizations were conducted on catalysts. Firstly, FT-IR was used to analyze the characteristic adsorption peaks of the spectra of KOH/ $\text{SiO}_2$ ,  $\text{SiO}_2$ , KOH/diatomite and pure diatomite (As shown in Fig. 1). Among the multi-peaks, the spectral peaks at the position of ca. 1630 /810 /790  $\text{cm}^{-1}$  and 3430  $\text{cm}^{-1}$  can be related to the symmetric stretching and out of plane bending vibrations of Si-O-Si, -OH, respectively<sup>[20]</sup>. Thus, all samples contain the Si-O-Si and -OH groups. The major difference of KOH/diatomite and KOH/ $\text{SiO}_2$  are described as following: (i)

In KOH/diatomite, a new obvious peak is observed visible at ca.  $1440\text{ cm}^{-1}$ , which is owing to K-O-Si group stretching vibration <sup>[21]</sup>; (ii) In KOH/SiO<sub>2</sub>, a peak appeared at the position of ca.  $621\text{ cm}^{-1}$ , which can be ascribed to the existence of Si-H stretching vibration and this group differs from others. Above-mentioned indicates that both diatomite and SiO<sub>2</sub> react with KOH after KOH loading. However, different substances are formed. In addition, to further investigate the effect of calcination on the catalyst, KOH/diatomite catalyst without calcination was also prepared and named as KOH/diatomite-UC. Based on the FT-IR analysis carried on KOH/diatomite-UC, a new absorption peak is observed visible at ca.  $899/1383\text{ cm}^{-1}$ , which is denoting the Si-OH functional group. The formation of this group could be attributed to the absorbed moisture during mix process. After calcination, this signal disappeared and the absorption peak of  $1440\text{ cm}^{-1}$  enhanced, which revealed that the Si-OH was transformed to K-O-Si group during calcination.

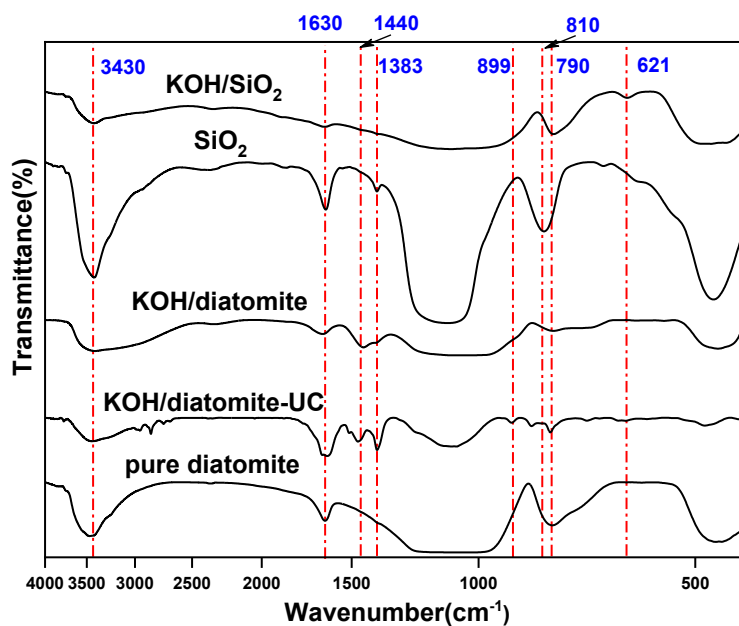


**Figure 1.** The FT-IR spectra of KOH/SiO<sub>2</sub>, SiO<sub>2</sub>, KOH/diatomite, KOH/diatomite-UC and pure diatomite.

Subsequently, X-ray diffraction (XRD) was performed (As shown in Fig. 2 (a) and Fig. S1). XRD patterns of both fumed SiO<sub>2</sub> and diatomite exhibited amorphous SiO<sub>2</sub> structure. After KOH loading, the diffraction peak of KOH/diatomite became wider and lower than pure diatomite. This indicates that KOH is well-distributed over the diatomite support with amorphous structure maintaining. However, the intensity of SiO<sub>2</sub> diffraction peak of KOH/SiO<sub>2</sub> was obviously enhanced. This situation is closely associated with following facts that fumed, amorphous SiO<sub>2</sub> was dehydrated and transformed to crystalline SiO<sub>2</sub> during this process. To further verify the above hypothesis, a new catalyst (KOH/diatomite-AW catalyst) was prepared and tested (As shown in Fig. S3-S5). During the mix process of this catalyst, 10 wt.% additional water was added. As was expected, compared with KOH/diatomite, the activity of KOH/diatomite-AW catalyst was declined. According to the FT-IR result, the spectra of KOH/diatomite-AW catalyst becomes similar with KOH/SiO<sub>2</sub>: the absorption peak of 1440 cm<sup>-1</sup>, which is attributed to the K-O-Si active site, is reduced obviously. This above phenomenon indicates that absorbed water may be the root cause of this catalytic difference.

However, there were still some diffraction peaks (ca. 26°-35°) with low intensity which cannot be attributed in KOH/SiO<sub>2</sub> and KOH/diatomite-AW. To get deep insight of this signal which may disclose the interaction between KOH and SiO<sub>2</sub> during this

process, high KOH loading KOH/SiO<sub>2</sub> (2:1) was prepared and characterized. According to the result, new peaks have occurred both KHSiO<sub>3</sub> and K<sub>2</sub>Si<sub>4</sub>O<sub>9</sub> were identified as major products. Based on this result and FT-IR spectra of KOH/SiO<sub>2</sub>, diffraction peaks (ca. 26°-35°) of KOH/SiO<sub>2</sub> can be attributed to these two types of silicates, e.g. KHSiO<sub>3</sub> and K<sub>2</sub>Si<sub>4</sub>O<sub>9</sub>. According to the literature, (1) K<sub>2</sub>Si<sub>4</sub>O<sub>9</sub> is a stable, glass type of wadeite mineral containing high (4-6) coordinated Si atoms [22]. However, medium or strong solid basic/acid sites are necessary for cyclopentanone self-condensation [23], which K<sub>2</sub>Si<sub>4</sub>O<sub>9</sub> does not possess. (2) KHSiO<sub>3</sub> is not stable and can be transformed to colloidal type (OH)<sub>2</sub>SiO<sub>2</sub><sup>2-</sup> component in water [24]. It is inevitable that KHSiO<sub>3</sub> component can absorb water either from air or during reaction. The visible alterations of appearance of used KOH/SiO<sub>2</sub> catalyst is also in agreement with this (As shown in Fig. S2). Thus, the poor activity of KOH/SiO<sub>2</sub> can be reasonably linked to the inactive and unstable K<sub>2</sub>Si<sub>4</sub>O<sub>9</sub> and KHSiO<sub>3</sub> components in KOH/SiO<sub>2</sub> catalyst. In addition, the XRD data illustrated that KOH/diatomite-AW maintained amorphous structure (As shown in Fig. S5). However, as similar with KOH/SiO<sub>2</sub> catalyst, some diffraction peaks with low intensity appeared in ca. 26°-35°. It can be assumed from this result that inactive and unstable K<sub>2</sub>Si<sub>4</sub>O<sub>9</sub> and KHSiO<sub>3</sub> components were synthesized in KOH/diatomite-AW catalyst, which may decrease the catalytic activity directly.

TGA results were also consistent with XRD and FT-IR results as shown in Fig. 2 (b). The weight loss of KOH/diatomite could be explained by evaporation of water (~100 °C), formation of K-O-Si group (~200 °C) and reached stable above 300 °C. For KOH/SiO<sub>2</sub>,

the obvious decrease ( $\sim 100\text{ }^{\circ}\text{C}$ ) was related to the dehydration of fumed  $\text{SiO}_2$  and the slight and long-range reduction ( $>100\text{ }^{\circ}\text{C}$ ) may be attributed to the transformation of KOH and formation of  $\text{K}_2\text{Si}_4\text{O}_9$  and  $\text{KHSiO}_3$ .

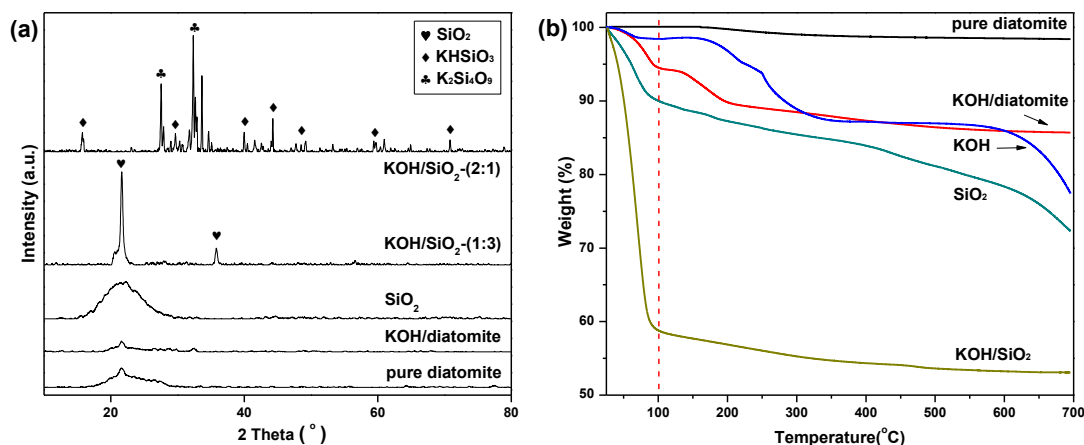


**Figure 2.** (a) XRD pattern and (b) TGA analysis of pure diatomite, KOH/diatomite,  $\text{SiO}_2$  and KOH/ $\text{SiO}_2$ .

Furthermore, the BET surface areas, total pore volume and pore size areas distribution of catalysts are summarized in Table. 1, and SEM analysis is showed in Fig. S6. Based on the analysis results, there was obvious difference between these two supports. For diatomite, the surface area increased markedly from  $13.11\text{ m}^2\text{ g}^{-1}$  to  $22.27\text{ m}^2\text{ g}^{-1}$ . Whereas, the surface area of  $\text{SiO}_2$  fell sharply from  $205.02\text{ m}^2\text{ g}^{-1}$  to only  $10.04\text{ m}^2\text{ g}^{-1}$  after KOH loading. KOH/diatomite possessed higher surface area, larger pore volume and pore size. It can be assumed that KOH was well-distributed into diatomite compared with KOH/ $\text{SiO}_2$ . These results were corroborated with XRD results (Fig. 2(a)) and SEM images (Fig. S6). Namely, KOH was well-distributed over the diatomite support with amorphous structure maintaining, but fumed amorphous  $\text{SiO}_2$  was dehydrated and transformed to crystalline  $\text{SiO}_2$ .

**Table 1.** BET surface areas, total pore volume and pore size areas of the support or catalyst.

<b>Support or catalyst</b>	<b>BET surface areas (m<sup>2</sup> g<sup>-1</sup>)</b>	<b>Pore volume (cm<sup>3</sup> g<sup>-1</sup>)</b>	<b>Pore size areas(nm)</b>
diatomite	13.11	0.012	5.49
KOH/diatomite	22.27	0.028	17.75
SiO <sub>2</sub>	205.02	0.572	11.43
KOH/SiO <sub>2</sub>	10.04	0.004	3.70

To confirm the dispersity of KOH/SiO<sub>2</sub> and KOH/diatomite catalysts, SEM-EDS analysis was conducted and presented in Fig. 3. According to the results, the EDS mapping of (a) KOH/SiO<sub>2</sub> and (b) KOH/diatomite both showed that K, Si, O elements were detected on support with well dispersity. Moreover, Al<sub>2</sub>O<sub>3</sub> (5.10%), Na<sub>2</sub>O (0.33%), CaO (0.30%) were found as minor impurity components over KOH/diatomite. According to the literature, these minor components can also catalyze the reaction<sup>[25]</sup>. Thus, it can be concluded that there is synergistic effect between KOH and these impurity components of diatomite.

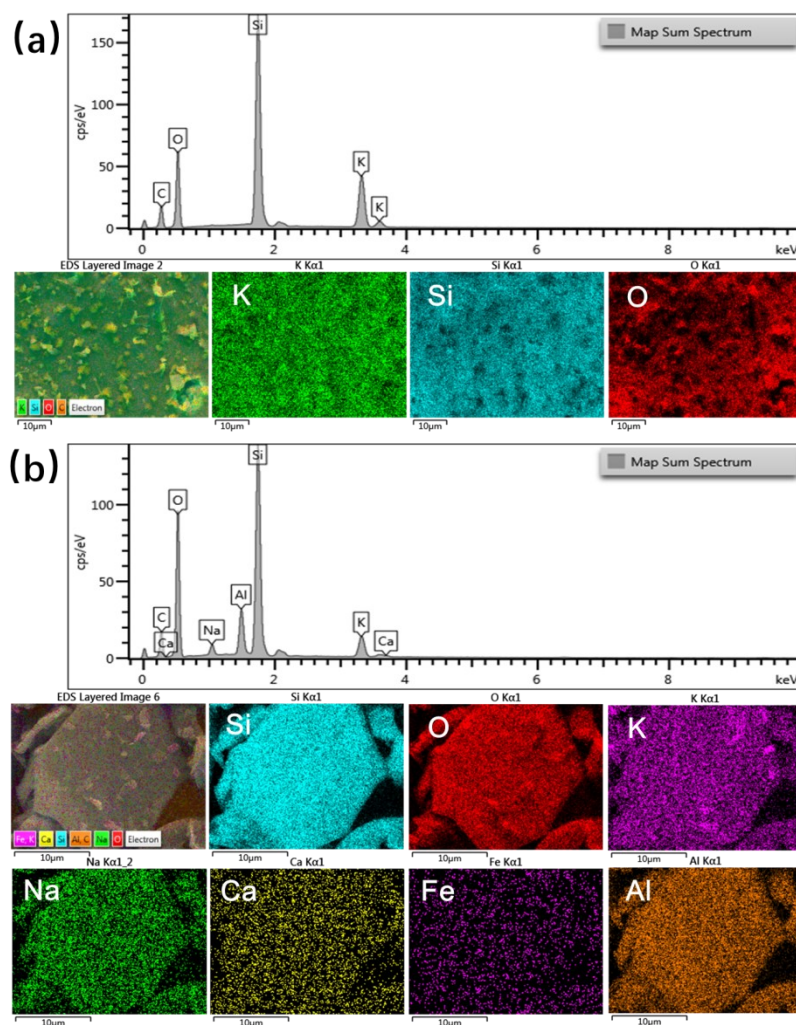


**Figure 3.** SEM images (magnification: 2000) with EDS mapping of (a) KOH/SiO<sub>2</sub> (b) KOH/diatomite with 500 °C calcination.

### 3.2 Catalytic Activity

To investigate the effect of KOH loading amount on diatomite for cyclopentanone self-condensation, various mass ratio of KOH/diatomite catalyst was designed in the experiment. Obviously, both conversion, total yield of dimer and trimer improved, while the KOH loadings changing from 1:6 to 1:1 (As shown in Fig. S7). However, the yield of trimer increased rapidly when KOH/diatomite mass ratio a further increase from 1:3 to 1:1, which led to the low selectivity of dimer. Based on a balance between dimer

yield and selectivity, KOH/diatomite-1:3 was selected as the optimized mass ratio of KOH/diatomite.

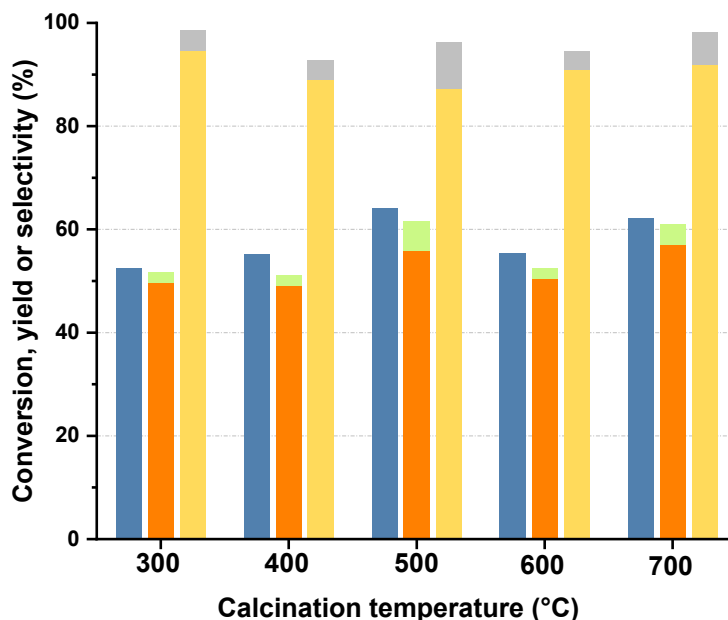


**Figure 4.** Effect of different calcination temperature of KOH/diatomite catalyst. Cyclopentanone conversion (blue bar), yield of **dimer** (orange bar) and **trimer** (green bar), selectivity of **dimer** (yellow bar) and **trimer** (gray bar) over KOH/diatomite catalyst. Reaction conditions: 1.0 g KOH/diatomite catalyst; 4.0 g cyclopentanone; 180 °C; 2 h.

Subsequently, the calcination temperature of KOH/diatomite was also investigated (As shown in Fig. 4). It is clear that the conversion, yield and selectivity did not change greatly over different calcination temperature. This result is consistent with TGA and XRD (As shown in Fig. 2 (b) and Fig. S1) results. The weight loss of KOH/diatomite reached stable above 300 °C. XRD results illustrated that no significantly difference was detected on different calcination temperature of KOH/diatomite catalysts.

Figure 5 shows the activity comparison of KOH/SiO<sub>2</sub> and KOH/diatomite catalysts. Unexpectedly, under KOH/SiO<sub>2</sub> catalyst, there was no cyclopentanone conversion with three repeated experiments conducted. While KOH/diatomite catalyst exhibited relatively high dimer yield (55.9%) under the same reaction conditions. It can be inferred from this result that diatomite support is more suitable for KOH than commercial SiO<sub>2</sub>. Meanwhile, above characterizations of FT-IR, SEM-EDS and BET have explained the reason of obviously different catalytic activity. we suggest that the excellent activity of KOH/diatomite catalyst can be attributed to the formation of K-O-Si bond. In addition, the impurity elements existed in diatomite (e.g. CaO, Na<sub>2</sub>O, Al<sub>2</sub>O<sub>3</sub>) and higher BET surface areas may also benefit to this reaction.

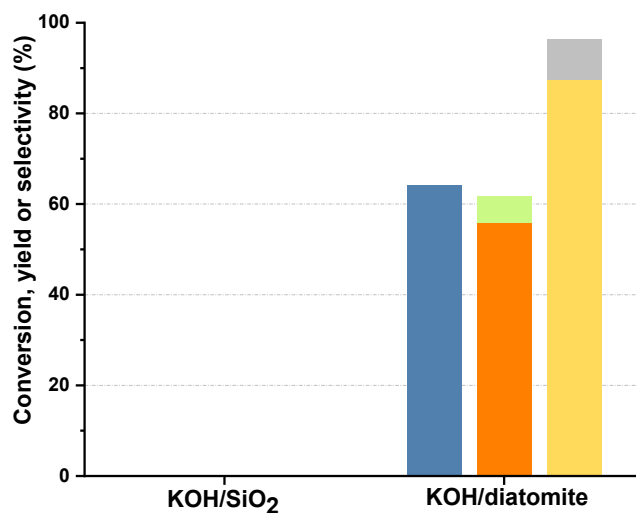


**Figure 5.** Comparison of KOH/SiO<sub>2</sub> and KOH/diatomite catalysts.

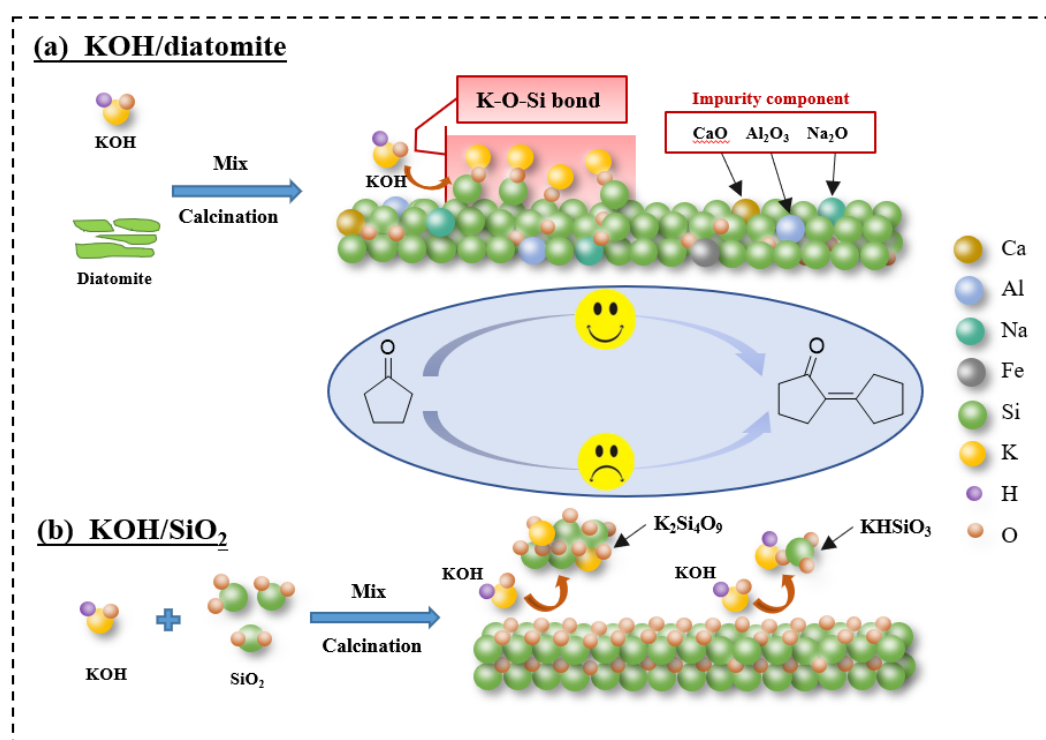
Cyclopentanone conversion (blue bar), yield of **dimer** (orange bar) and **trimer** (green bar), selectivity of **dimer** (yellow bar) and **trimer** (gray bar) over KOH/diatomite

catalyst. Reaction conditions: 1.0 g KOH/support catalyst (KOH/support=1:3); 4.0 g cyclopentanone; 180 °C; 2 h; 500 °C calcination.

To improve the yield of dimer, reaction time was extended from 2 h to 8 h (As shown in Fig. S8). With the extension of reaction time, the total yield improved to 85.0%, which is relatively high for catalytic reaction. Furthermore, the reusability of catalyst is crucial parameter to assess catalytic activity for reaction. Thus, reusability test of KOH/diatomite catalyst was carried out (As shown in Fig. S9). Dimer yield declined slightly after three runs, but there is no significant microstructure difference among KOH/diatomite catalyst after three times reaction cycles (As shown in Fig. S10). Based on the XRD results of spent catalysts, the diffraction peaks (ca. 26°-35°) were appeared (As shown in Fig. S11), which were similar to the inactive and unstable  $K_2Si_4O_9$  and  $KHSiO_3$  components in KOH/SiO<sub>2</sub> catalyst. This inactivation may be caused by the H<sub>2</sub>O generated during reaction. Compared to KOH aqueous solution, KOH/diatomite heterogeneous catalyst exhibited reusability and was more environmentally friendly. Based on this result, the cost accounting of our KOH/diatomite catalyst and traditional KOH aqueous solution was conducted. Because of the reusability, the cost of KOH/diatomite catalyst decreases 47.0% at least (The calculative process was listed in Supporting information). According to the above cost benefit analysis, the use of KOH/diatomite catalyst is more economical and environmentally friendly than KOH aqueous solution.

On the basic of the catalytic evaluations and the overall structural characterizations, a

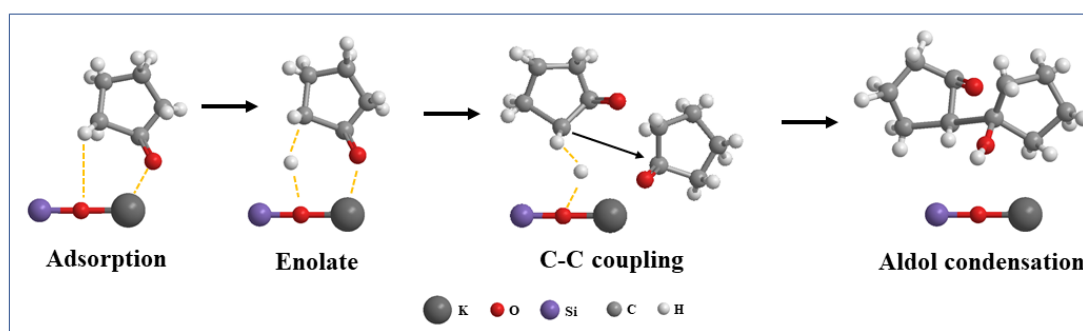
proposed catalyst synthesis pathway and reaction mechanism of KOH/diatomite and KOH/SiO<sub>2</sub> is showed in Scheme 1. For KOH/diatomite catalyst, K-O-Si bond was formed during dry-mixed impregnation process and identified as the active group for cyclopentanone self-condensation. Moreover, the minor impurity components (e.g. CaO, Na<sub>2</sub>O, Al<sub>2</sub>O<sub>3</sub>) in diatomite may also benefit to this reaction. However, for KOH/SiO<sub>2</sub> catalyst, inactive and unstable K<sub>2</sub>Si<sub>4</sub>O<sub>9</sub> and KHSiO<sub>3</sub> were formed during preparation process, which led to the inactivation of the reaction.



**Scheme 1.** Proposed catalyst synthesis and reaction pathway of KOH/diatomite and KOH/SiO<sub>2</sub>.

Furthermore, a proposed reaction mechanism for cyclopentanone aldol condensation on K-O-Si bond is showed in Scheme 2. It is well-known that aldol condensation of cyclopentanone is an effective reaction for C–C coupling with simultaneous elimination

of O-atom. Meanwhile, the elementary steps include the following sequence of steps: adsorption of reactants, enolization/ $\alpha$ -C-H abstraction, C-C coupling, dehydration and desorption to the final  $\alpha$ ,  $\beta$ -unsaturated oxygenates. As shown in Scheme 2, due to the acidic of carbonyl compounds, the basic O anion are able to abstract the  $\alpha$ -C-H from the ketone and forms an enolate, which is stabilized by delocalizing the negative charge onto an electronegative O. Then, the enolate was formed in this base-route which could readily attack another carbonyl to form a C-C bond, because of the negatively charged. In this step, the second carbonyl can be either adsorbed on a vicinal K-cation or from the liquid phase as shown below.



**Scheme 2.** Proposed reaction mechanism for cyclopentanone aldol condensation on K-O-Si bond.

#### 4. Conclusions

This work presents the synthesis and characterization of a heterogeneous diatomite stabilized KOH catalyst and exhibited relatively high yield (85.0% total yield) and good reusability. Through multiple characterizations, it can be noticed that KOH is well-distributed over the diatomite support with amorphous structure maintaining. The

excellent catalytic activity of KOH/diatomite can be attributed to the formation of K-O-Si bond as active site. In addition, the impurity elements existed in diatomite (e.g. CaO, Na<sub>2</sub>O, Al<sub>2</sub>O<sub>3</sub>) and higher BET surface areas may also benefit to this reaction. Compared to KOH aqueous solution, KOH/diatomite heterogeneous catalyst exhibited good reusability and was more environmentally friendly. Because of the reusability, the cost of KOH/diatomite catalyst decreases 47.0% at least. Meanwhile, this work may demonstrate a new approach to stabilization KOH on heterogeneous support by using natural diatomite and has a significant fall in catalyst cost compared with traditional homogeneous KOH catalyst.

**Author Contributions:**

Qianqian Xu performed the experiments; Na Li, Jian Zhang, Meihong Niu and Haiqiang Shi analyzed the data; Qingwei Ping contributed reagents and analysis tools; and Xueru Sheng conceived, designed the experiments and reviewed the paper.

**Acknowledgments:**

This work was supported by National Natural Science Foundation of China [No. 21808023]; Natural Science Foundation of Liaoning [No. 20180550559]; Liaoning Revitalization Talents Program [XLYC1802025].

**Conflicts of Interest:**

The authors declare no conflict of interest.

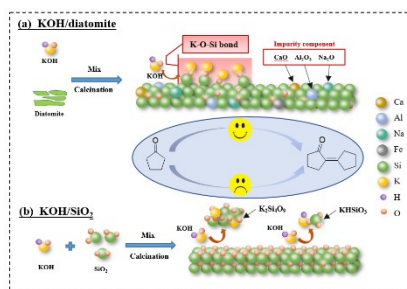
**Indicate:**

The color should be used for figures in print.

## References:

- [1] a) A. Corma, S. Iborra, A. Velty, *Chem. Rev.* **2007**, *107*, 2411-2502; b) G. Li, B. Hou, A. Wang, X. Xin, Y. Cong, X. Wang, N. Li, T. Zhang, *Angew. Chem. Int. Ed. Engl.* **2019**, *58*, 12154-12158; c) C. Jia, C. Chen, R. Mi, T. Li, J. Dai, Z. Yang, Y. Pei, S. He, H. Bian, S. H. Jang, J. Y. Zhu, B. Yang, L. Hu, *ACS Nano* **2019**, *13*, 9993-10001; d) M. Shahabuddin, M. T. Alam, B. B. Krishna, T. Bhaskar, G. Perkins, *Bioresource Technol.* **2020**, *312*, 123596; e) O. Kikhtyanin, D. Kadlec, R. Velvarská, D. Kubička, *ChemCatChem* **2018**, *10*, 1464-1475.
- [2] a) J. Yang, S. Li, N. Li, W. Wang, A. Wang, T. Zhang, Y. Cong, X. Wang, G. W. Huber, *Ind. Eng. Chem. Res.* **2015**, *54*, 11825-11837; b) C. A. Scaldaferrri, V. M. D. Pasa, *Chem. Eng. J.* **2019**, *370*, 98-109.
- [3] a) C. Gutiérrez-Antonio, F. I. Gómez-Castro, J. A. de Lira-Flores, S. Hernández, *Renew. Sust. Energ. Rev.* **2017**, *79*, 709-729; b) J. Y. Kim, H. W. Lee, S. M. Lee, J. Jae, Y. K. Park, *Bioresource Technol.* **2019**, *279*, 373-384; c) G. W. Diederichs, M. Ali Mandegari, S. Farzad, J. F. Gorgens, *Bioresource Technol.* **2016**, *216*, 331-339; d) H. Li, A. Riisager, S. Saravanamurugan, A. Pandey, R. S. Sangwan, S. Yang, R. Luque, *ACS Catal.* **2017**, *8*, 148-187; e) J. Li, J. Sun, R. Fan, Y. Yoneyama, G. Yang, N. Tsubaki, *ChemCatChem* **2017**, *9*, 2668-2674.
- [4] a) E. L. Kunkes, D. A. Simonetti, R. M. West, J. C. Serrano-Ruiz, C. A. Gärtner, J. A. Dumesic, *Science* **2008**, *322*, 417; b) Y. Román-Leshkov, C. J. Barrett, Z. Y. Liu, J. A. Dumesic, *Nature* **2007**, *447*, 982-985.
- [5] a) G. W. Huber, J. N. Chheda, C. J. Barrett, J. A. Dumesic, *Science* **2005**, *308*, 1446-1450; b) J. Q. Bond, A. A. Upadhye, H. Olcay, G. A. Tompsett, J. Jae, R. Xing, D. M. Alonso, D. Wang, T. Zhang, R. Kumar, A. Foster, S. M. Sen, C. T. Maravelias, R. Malina, S. R. H. Barrett, R. Lobo, C. E. Wyman, J. A. Dumesic, G. W. Huber, *Energy Environ. Sci.* **2014**, *7*, 1500-1523.
- [6] a) A. Corma, O. de la Torre, M. Renz, N. Villandier, *Angew. Chem. Int. Ed. Engl.* **2011**, *50*, 2375-2378; b) K. S. Arias, M. J. Climent, A. Corma, S. Iborra, *Energy Environ. Sci.* **2015**, *8*, 317-331.
- [7] a) Q.-N. Xia, Q. Cuan, X.-H. Liu, X.-Q. Gong, G.-Z. Lu, Y.-Q. Wang, *Angew. Chem. Int. Ed. Engl.* **2014**, *53*, 9755-9760; b) N. Luo, T. Montini, J. Zhang, P. Fornasiero, E. Fonda, T. Hou, W. Nie, J. Lu, J. Liu, M. Heggen, L. Lin, C. Ma, M. Wang, F. Fan, S. Jin, F. Wang, *Nat. Energy* **2019**, *4*, 575-584; c) Y. Liu, G. Li, Y. Hu, A. Wang, F. Lu, J.-J. Zou, Y. Cong, N. Li, T. Zhang, *Joule* **2019**, *3*, 1028-1036.
- [8] a) Y. Yang, Z. Du, Y. Huang, F. Lu, F. Wang, J. Gao, J. Xu, *Green Chem.* **2013**, *15*, 1932-1940; b) R. Fang, H. Liu, R. Luque, Y. Li, *Green Chem.* **2015**, *17*, 4183-4188; c) Y. Wang, S. Sang, W. Zhu, L. Gao, G. Xiao, *Chem. Eng. J.* **2016**, *299*, 104-111.
- [9] J. Cueto, L. Faba, E. Díaz, S. Ordóñez, *ChemCatChem* **2017**, *9*, 1765-1770.
- [10] W. Wang, N. Li, G. Li, S. Li, W. Wang, A. Wang, Y. Cong, X. Wang, T. Zhang, *ACS Sustain. Chem. Eng.* **2017**, *5*, 1812-1817.
- [11] Q. Deng, G. Nie, L. Pan, J.-J. Zou, X. Zhang, L. Wang, *Green Chem.* **2015**, *17*, 4473-4481.
- [12] J. Yang, N. Li, G. Li, W. Wang, A. Wang, X. Wang, Y. Cong, T. Zhang, *Chem. Commun.* **2014**, *50*, 2572-2574.
- [13] D. Liang, G. Li, Y. Liu, J. Wu, X. Zhang, *Catal. Commun.* **2016**, *81*, 33-36.
- [14] a) X. Qi, M. Liu, Z. Chen, R. Liang, *Polym. Advan. Technol.* **2007**, *18*, 184-193; b) S. Martinovic,

- M. Vlahovic, T. Boljanac, L. Pavlovic, *Int. J. Miner. Process.* **2006**, *80*, 255-260; c) I. Kashcheev, A. Popov, S. Ivanov, *Refract. Ind. Ceram+* **2009**, *50*, 98-100; d) H. Bakr, *Asian J. Mater. sci.* **2010**, *2*, 121-136.
- [15] a) K. Wang, Z. Tang, W. Wu, P. Xi, D. Liu, Z. Ding, X. Chen, X. Wu, S. Chen, *Electrochim. Acta* **2018**, *284*, 119-127; b) Q. Li, G. Zhai, Y. Xu, T. Odoom-Wubah, L. Jia, J. Huang, D. Sun, Q. Li, *Ind. Eng. Chem. Res.* **2019**, *58*, 14008-14015.
- [16] Z. Zhang, Z. Wang, *J. org. chem.* **2006**, *71*, 7485-7487.
- [17] R. Shan, C. Zhao, H. Yuan, S. Wang, Y. Wang, *Energ. Convers. Manage.* **2017**, *138*, 547-555.
- [18] A. M. Rabie, M. Shaban, M. R. Abukhadra, R. Hosny, S. A. Ahmed, N. A. Negm, *J. Mol. Liq.* **2019**, *279*, 224-231.
- [19] B. Wang, F. Li, P. Yang, Y. Yang, J. Hu, J. Wei, Q. Yu, *J. Chem. Eng. Data* **2018**, *64*, 360-371.
- [20] A. B. D. Nandiyanto, N. Permatasari, T. N. Sucahya, A. G. Abdullah, L. Hasanah, *Mat. Sci. Eng.* **2017**, *180*.
- [21] E. Modiba, C. Enweremadu, H. Rutto, *Chinese J. Chem. Eng.* **2015**, *23*, 281-289.
- [22] a) J. R. Allwardt, B. C. Schmidt, J. F. Stebbins, *Chem. Geol.* **2004**, *213*, 137-151; b) N. Kinomura, S. Kume, M. Koizumi, in *proceedings of the 4 th international conference of high pressure scientific technique, Vol. 211*, **1975**, p. 214.
- [23] X. Sheng, G. Li, W. Wang, Y. Cong, X. Wang, G. W. Huber, N. Li, A. Wang, T. Zhang, *AICHE J.* **2016**, *62*, 2754-2761.
- [24] X. Yuan, S. Fan, S. W. Choi, H.-T. Kim, K. B. Lee, *Appl. Energ.* **2017**, *195*, 850-860.
- [25] X. Sheng, Q. Xu, X. Wang, N. Li, H. Jia, H. Shi, M. Niu, J. Zhang, Q. Ping, *Catalysts* **2019**, *9*, 661.



**Scheme 1.** Proposed catalyst synthesis and reaction pathway of KOH/diatomite and KOH/SiO<sub>2</sub>.

**Key words:**

Biomass; Diatomite; Heterogeneous catalysts; KOH; Self-condensation

A heterogeneous catalyst (KOH/diatomite) was prepared in a simple way, and exhibited good activity (overall yield: 85.0%). We suggest that the excellent catalytic activity of KOH/diatomite can be attributed to the formation of K-O-Si bond, the impurity elements existed in diatomite and higher BET surface areas may also benefit.